Flavor Violating Higgs Couplings in Minimal Flavor Violation

Min He

Shanghai Jiao Tong University, Shanghai, China
arXiv:1807.00921 (submitted to JHEP)
Collaborators: Xiao-Gang He, Xing-Bo Yuan, and Jin-Jun Zhang

Nov. 26 - 30, 2018
Higgs Couplings 2018, Tokyo

Outline

Section 1

Motivation

Motivation

Higgs boson has been discovered in 2012! What's next?

- Precision measurements on the Higgs couplings with the SM particles will be one of the most important tasks for the LHC Run II and its high-luminosity upgrade.
- A significant deviation from the SM expectations in Higgs phenomenology would be an indicator of new physics.
- Recent measurements on $h \to \ell_1 \ell_2$, $B_{s,d} \to \ell_1 \ell_2$, $\mu \to e\gamma$ and $\mu \to e$ conversion in nuclei motivated us to study Higgs FCNC couplings.
- Especially emphasize on the Higgs FCNC couplings in Minimal Flavor Violation hypothesis which could naturally explain the smallness of these flavor violating couplings.

Section 2

Higgs FCNC couplings

Higgs FCNC couplings: General case

The Higgs FCNC Yukawa couplings appear in many extensions of the SM in the Higgs sector, such as multi-Higgs doublet models. In this work, we will not go into detailed model studies of these FCNC couplings but adopt an EFT approach to use known data to obtain model independent constraints on them.

- In the SM, the Yukawa interactions

$$-\mathcal{L}_Y = \bar{Q}_L H Y_d d_R + \bar{Q}_L \tilde{H} Y_u u_R + \text{h.c.}, \tag{1}$$

- Considering the BSM effects in the EFT approach, these Higgs Yukawa interactions can be affected by dim-6 operators at the tree level.

Higgs FCNC couplings: General case

We will work in the Warsaw basis [Grazdkowski, etc., 2010]. There exist only three operators relevant to our analysis to the lowest order.

$$\begin{aligned}\mathcal{O}_{dH} &= (H^\dagger H)(\bar{Q}_L H C_{dH} d_R),\\ \mathcal{O}_{uH} &= (H^\dagger H)(\bar{Q}_L \tilde{H} C_{uH} u_R),\\ \mathcal{O}_{\ell H} &= (H^\dagger H)(\bar{L}_L H C_{\ell H} e_R),\end{aligned} \tag{2}$$

After the symmetry breaking $H^\dagger H \to 1/2v^2$, the Yukawa couplings of h to fermions are given by

$$\mathcal{L}_Y^f = -\frac{1}{\sqrt{2}}\bar{f}_L \bar{Y}_f f_R v - \frac{1}{\sqrt{2}}\bar{f}_L\left(\bar{Y}_f - \frac{v^2}{\Lambda^2}C_{fH}\right) f_R h + \text{h.c.}\,. \tag{3}$$

with the definition

$$\bar{Y}_f = Y_f - \frac{1}{2}\frac{v^2}{\Lambda^2}C_{fH}, \tag{4}$$

where Λ denotes some NP scale.

Higgs FCNC couplings: General case

In the mass-eigenstate basis $\bar{Y}_f$ becomes diagonal, but the Higgs Yukawa interactions $(1/\sqrt{2})(\bar{Y}_f - (v^2/\Lambda^2)C_{fH})$ is in general not diagonal and induces FCNC interactions. We write them as

$$\mathcal{L}_Y = -\frac{1}{\sqrt{2}}\bar{f}(Y_L P_L + Y_R P_R) f h, \tag{5}$$

where Y_L and Y_R are 3×3 complex matrices in flavor space and connect to each other by the relation $Y_L = Y_R^\dagger$. In the literature, the following basis for the Higgs Yukawa interactions is also widely used

$$\mathcal{L}_Y = -\frac{1}{\sqrt{2}}\bar{f}(Y + i\gamma_5 \bar{Y}) f h\,. \tag{6}$$

Here, Y and $\bar{Y}$ are 3×3 Hermitian matrices. This form is related to eq. (5) by $Y_{R,L} = Y \pm i\bar{Y}$.

Higgs FCNC couplings: Within Minimal Flavor Violation

In the SM, the Yukawa interactions in eq. (1) violate the global flavor symmetry

$$G_{\rm QF} = SU(3)_{Q_L} \otimes SU(3)_{u_R} \otimes SU(3)_{d_R} \,. \tag{7}$$

This flavor symmetry can be recovered by formally promoting the Yukawa matrices to spurions fields, which transform as

$$Y_u \sim (\mathbf{3}, \bar{\mathbf{3}}, \mathbf{1}) \qquad \text{and} \qquad Y_d \sim (\mathbf{3}, \mathbf{1}, \bar{\mathbf{3}}). \tag{8}$$

Then, two basic building block spurions A $\equiv Y_u Y_u^\dagger$ and B $\equiv Y_d Y_d^\dagger$ under the group $SU(3)_{Q_L} \otimes SU(3)_{u_R} \otimes SU(3)_{d_R}$ transforming as $(\mathbf{1}+\mathbf{8}, \mathbf{1}, \mathbf{1})$ are important to parametrize the FCNC Yukawa couplings.

Higgs FCNC couplings: Within Minimal Flavor Violation

MFV hypothesis implies that, all CP and flavor violating sources come from $Y_{u,d}$ and the effective Lagrangian is invariant under the flavor symmetry group $G_{\rm QF}$. Therefore $C_{uH,dH}$ can be written in the following form,

$$C_{dH} = f_d(\mathsf{A},\mathsf{B})Y_d \quad \text{and} \quad C_{uH} = f_u(\mathsf{A},\mathsf{B})Y_u\,. \tag{9}$$

The function $f_{u,d}(\mathsf{A},\mathsf{B})$ can be expanded in an infinite series of the form $f_{u,d}(\mathsf{A},\mathsf{B}) \equiv \xi^{u,d}_{ijk\cdots}\mathsf{A}^i\mathsf{B}^j\mathsf{A}^k\cdots$ with $\xi^{u,d}_{ijk\cdots}$ to be real since no new CP violating source should be introduced other than that already contained in $Y_{u,d}$. Using the Cayley-Hamilton identity, $f(\mathsf{A},\mathsf{B})$ can be generally resumed into 17 terms,

$$\begin{aligned}\kappa_1\mathbb{1}&+\kappa_2\mathsf{A}+\kappa_5\mathsf{B}^2+\kappa_6\mathsf{AB}+\kappa_8\mathsf{ABA}+\kappa_{11}\mathsf{AB}^2+\kappa_{13}\mathsf{A}^2\mathsf{B}^2+\kappa_{15}\mathsf{B}^2\mathsf{AB}+\kappa_{16}\mathsf{AB}^2\mathsf{A}^2\\ &+\kappa_3\mathsf{B}+\kappa_4\mathsf{A}^2+\kappa_7\mathsf{BA}+\kappa_{10}\mathsf{BAB}+\kappa_9\mathsf{BA}^2+\kappa_{14}\mathsf{B}^2\mathsf{A}^2+\kappa_{12}\mathsf{ABA}^2+\kappa_{17}\mathsf{B}^2\mathsf{A}^2\mathsf{B}\end{aligned}$$

$\mathrm{Im}\kappa_i \propto |\mathrm{Tr}(\mathsf{A}^2\mathsf{BAB}^2)| \ll 1$, these tiny imaginary parts can be neglected.

Higgs FCNC couplings: Within Minimal Flavor Violation

Since the spurion B is highly suppressed by the small down-type quark Yukawa couplings, terms with B are neglected and we obtain

$$f_u(\mathsf{A},\mathsf{B}) \approx \epsilon_0^u \mathbb{1} + \epsilon_1^u \mathsf{A} + \epsilon_2^u \mathsf{A}^2 \quad \text{and} \quad f_d(\mathsf{A},\mathsf{B}) \approx \epsilon_0^d \mathbb{1} + \epsilon_1^d \mathsf{A} + \epsilon_2^d \mathsf{A}^2 \,. \tag{10}$$

For the lepton sector in type-I seesaw mechanism, the basic building block spurion reads in the mass eigenstate

$$\mathsf{A}_\ell = \frac{2\mathcal{M}}{v^2} U \hat{m}_\nu^{1/2} O O^\dagger \hat{m}_\nu^{1/2} U^\dagger \,, \tag{11}$$

where U denotes the PMNS matrix, and matrix O is generally complex orthogonal, satisfying $OO^T = \mathbb{1}$.

Higgs FCNC couplings: Within Minimal Flavor Violation

In summary, the Yukawa couplings in the MFV framework can be written as

$$
\begin{aligned}
Y_R^d &= (1-\hat{\epsilon}_0^d)\lambda_d - \hat{\epsilon}_1^d V^\dagger \lambda_u^2 V \lambda_d \,, \\
Y_R^u &= (1-\hat{\epsilon}_0^u)\lambda_u \,, \\
Y_R^\ell &= (1-\hat{\epsilon}_0^\ell)\lambda_\ell - \hat{\epsilon}_1^\ell \mathsf{A}_\ell \lambda_\ell - \hat{\epsilon}_2^\ell \mathsf{A}_\ell^2 \lambda_\ell,
\end{aligned} \tag{12}
$$

with Lagrangian in the form

$$
\mathcal{L}_Y = -\frac{1}{\sqrt{2}} \bar{f}(Y_L P_L + Y_R P_R) f h. \tag{13}
$$

Section 3

Relevant processes

Relevant processes: Neutral B and K meson mixing

Including the Higgs FCNC contributions, the effective Hamiltonian for $B_s - \bar{B}_s$ mixing can be written as [Buras, etc., 2001]

$$\mathcal{H}_{\rm eff}^{\Delta B=2} = \frac{G_F^2}{16\pi^2} m_W^2 (V_{tb}V_{ts}^*)^2 \sum_i C_i \mathcal{O}_i + \text{h.c.} \ , \tag{14}$$

where the operators are

$$\begin{aligned} \mathcal{O}_1^{\rm VLL} &= (\bar{s}^\alpha \gamma_\mu P_L b^\alpha)(\bar{s}^\beta \gamma^\mu P_L b^\beta) \ , \quad & \mathcal{O}_1^{\rm SLL} &= (\bar{s}^\alpha P_L b^\alpha)(\bar{s}^\beta P_L b^\beta) \ , \\ \mathcal{O}_2^{\rm LR} &= (\bar{s}^\alpha P_L b^\alpha)(\bar{s}^\beta P_R b^\beta) \ , & \mathcal{O}_1^{\rm SRR} &= (\bar{s}^\alpha P_R b^\alpha)(\bar{s}^\beta P_R b^\beta) \ , \end{aligned} \tag{15}$$

and the corresponding Wilson coefficients

$$\begin{aligned} C_1^{\rm SLL,NP} &= -\frac{1}{2}\tilde{\kappa}\left(Y_L^{sb}\right)^2 \ , \quad & C_2^{\rm LR,NP} &= -\tilde{\kappa} Y_L^{sb} Y_R^{sb} \ , \\ C_1^{\rm SRR,NP} &= -\frac{1}{2}\tilde{\kappa}\left(Y_R^{sb}\right)^2 \ , & \tilde{\kappa} &= \frac{8\pi^2}{G_F^2}\frac{1}{m_h^2 m_W^2}\frac{1}{(V_{tb}V_{ts}^*)^2} \ . \end{aligned} \tag{16}$$

Relevant processes: Neutral B and K meson mixing

The contribution from $\mathcal{H}_{\rm eff}^{\Delta B=2}$ to the transition matrix element of $B_s - \bar{B}_s$ mixing is given by,

$$M_{12}^s = \langle B_s | \mathcal{H}_{\rm eff}^{\Delta B=2} | \bar{B}_s \rangle = \frac{G_F^2}{16\pi^2} m_W^2 (V_{tb} V_{ts}^*)^2 \sum C_i \langle B_s | \mathcal{O}_i | \bar{B}_s \rangle \,, \quad (17)$$

where recent lattice calculations of the hadronic matrix elements $\langle \mathcal{O}_i \rangle$ can be found in some refs. Then the mass difference and CP violation phase read

$$\Delta m_s = 2 |M_{12}^s| \,, \qquad \text{and} \qquad \phi_s = \arg M_{12}^s \,. \quad (18)$$

Relevant processes: $B_s \to \ell_1 \ell_2$ decay

The effective Hamiltonian of the $B_s \to \mu^+\mu^-$ decay reads [Buchalla, etc., 1996]

$$\mathcal{H}_{\rm eff} = -\frac{G_F}{\sqrt{2}}\frac{\alpha_e}{\pi s_W^2} V_{tb}V_{ts}^*\big(C_A\mathcal{O}_A + C_S\mathcal{O}_S + C_P\mathcal{O}_P + C_S'\mathcal{O}_S' + C_P'\mathcal{O}_P'\big) + \text{h.c.}$$

and the operators $\mathcal{O}_i^{(\prime)}$ are defined as

$$\begin{aligned}
\mathcal{O}_A &= \big(\bar{q}\gamma_\mu P_L b\big)\big(\bar{\mu}\gamma^\mu\gamma_5\mu\big)\ , \\
\mathcal{O}_S &= m_b\big(\bar{q}P_R b\big)\big(\bar{\mu}\mu\big)\ , & \mathcal{O}_P &= m_b\big(\bar{q}P_R b\big)\big(\bar{\mu}\gamma_5\mu\big)\ , \\
\mathcal{O}_S' &= m_b\big(\bar{q}P_L b\big)\big(\bar{\mu}\mu\big)\ , & \mathcal{O}_P' &= m_b\big(\bar{q}P_L b\big)\big(\bar{\mu}\gamma_5\mu\big)\ .
\end{aligned} \tag{20}$$

And the Wilson coefficient

$$C_A^{\rm SM}(\mu_b) = -0.4690\left(\frac{m_t^{\rm P}}{173.1\ \text{GeV}}\right)^{1.53}\left(\frac{\alpha_s(m_Z)}{0.1184}\right)^{-0.09}\ , \tag{21}$$

and $C_S^{\rm SM} = C_S'^{\rm SM} = C_P^{\rm SM} = C_P'^{\rm SM} = 0$.

Relevant processes: $B_s \to \ell_1 \ell_2$ decay

The amplitudes P and S are defined as

$$P \equiv C_A + \frac{m_{B_s}^2}{2m_\mu}\left(\frac{m_b}{m_b+m_s}\right)(C_P - C_P')\,,$$
$$S \equiv \sqrt{1-\frac{4m_\mu^2}{m_{B_s}^2}}\frac{m_{B_s}^2}{2m_\mu}\left(\frac{m_b}{m_b+m_s}\right)(C_S - C_S')\,. \tag{22}$$

Due to the B_s-$\bar{B}_s$ oscillations, the measured branching ratio of $B_s \to \mu^+\mu^-$ should be the time-integrated one:

$$\bar{\mathcal{B}}(B_s \to \mu^+\mu^-) = \left(\frac{1+\mathcal{A}_{\Delta\Gamma} y_s}{1-y_s^2}\right)\mathcal{B}(B_s \to \mu^+\mu^-)\,, \tag{23}$$

with

$$y_s = \frac{\Gamma_s^{\rm L} - \Gamma_s^{\rm H}}{\Gamma_s^{\rm L} + \Gamma_s^{\rm H}} = \frac{\Delta\Gamma_s}{2\Gamma_s}, \mathcal{A}_{\Delta\Gamma} = \frac{|P|^2\cos(2\varphi_P - \phi_s^{\rm NP}) - |S|^2\cos(2\varphi_S - \phi_s^{\rm NP})}{|P|^2 + |S|^2} \tag{24}$$

Relevant processes: Leptonic decays $\ell_i \to \ell_j \gamma$

The effective Lagrangian for the $\ell_i \to \ell_j \gamma$ decays are given by [Harnik, etc., 2013]

$$\mathcal{L}_{\rm eff} = c_L \mathcal{O}_L + c_R \mathcal{O}_R + {\rm h.c.}, \tag{25}$$

with the operators

$$\mathcal{O}_{L,R} = \frac{e}{8\pi^2} m_i (\bar{\ell}_j \sigma^{\mu\nu} P_{L,R} \ell_i) F_{\mu\nu}\,, \tag{26}$$

where m_i denotes the mass of the lepton ℓ_i and $F_{\mu\nu}$ the photon field strength tensor. Then, the decay rate of $\ell_i \to \ell_j \gamma$ is given by

$$\Gamma(\ell_i \to \ell_j \gamma) = \frac{\alpha_e m_i^5}{64\pi^4} (|c_L|^2 + |c_R|^2). \tag{27}$$

The Wilson coefficients c_L and c_R receive contributions from the one-loop penguin diagrams. Their analytical expressions read

$$c_L^{1-\rm loop} = \sum_{f=e,\mu,\tau} F(m_i, m_f, m_j, 0, Y),\ c_R^{1-\rm loop} = \sum_{f=e,\mu,\tau} F(m_i, m_f, m_j, 0, Y^\dagger) \tag{28}$$

Relevant processes: Leptonic decays $\ell_i \to \ell_j \gamma$

The loop function reads

$$F(m_i, m_f, m_j, q^2, Y) = \frac{1}{8m_i} \int_0^1 dxdydz\delta(1-x-y-z) \frac{xzm_j Y_R^{jf} Y_L^{fi} + yzm_i Y_L^{jf} Y_R^{fi} + (x+y)m_f Y_L^{jf} Y_L^{fi}}{zm_h^2 - xzm_j^2 - yzm_i^2 + (x+y)m_f^2 - xyq^2}.$$

At the two-loop level, there are also comparable contributions from the Barr-Zee type diagrams. Here, we use the numerical results

$$\begin{aligned} c_L^{2-\text{loop}} &\approx \frac{1}{\sqrt{2}m_h^2} \frac{m_\tau}{m_i} Y_L^{ji}(-0.058 Y_R^{tt} + 0.11), \\ c_R^{2-\text{loop}} &\approx \frac{1}{\sqrt{2}m_h^2} \frac{m_\tau}{m_i} Y_R^{ji}(-0.058 Y_L^{tt} + 0.11), \end{aligned} \tag{29}$$

which are obtained from a full two-loop analytical calculations [Chang, etc., 1993]. Here, Y_L^{tt} and Y_R^{tt} are assumed to be real.

Relevant processes: $\mu \to e$ conversion in nuclei

The relevant effective Lagrangian reads [Harnik, etc., 2013]

$$\begin{aligned}\mathcal{L}_{\rm eff} =& c_L \frac{e}{8\pi^2} m_\mu (\bar{e}\sigma^{\mu\nu} P_L \mu) F_{\mu\nu} \\ &- \frac{1}{2}\sum_q \Big[g^q_{LS} (\bar{e} P_R \mu)(\bar{q} q) + g^q_{LV} (\bar{e}\gamma^\mu P_L \mu)(\bar{q}\gamma_\mu q) \Big] + \big(L \leftrightarrow R\big),\end{aligned} \tag{30}$$

The scalar operators are generated by the tree-level Higgs exchange and their Wilson coefficients are given by

$$g^q_{LS} = -\frac{1}{m_h^2} Y_R^{e\mu} {\rm Re}(Y_R^{qq}), \qquad g^q_{RS} = -\frac{1}{m_h^2} Y_L^{e\mu} {\rm Re}(Y_R^{qq}). \tag{31}$$

The corresponding Wilson coefficients read

$$g^q_{LV} = -\frac{\alpha_e Q_q}{2\pi q^2} \sum_{f=e,\mu,\tau} [G(m_\mu, m_f, m_e, q^2, Y) - G(m_\mu, m_f, m_e, 0, Y)], \tag{32}$$

Relevant processes: $\mu \to e$ conversion in nuclei

with the loop function

$$
\begin{aligned}
&G(m_i, m_f, m_j, q^2, Y) \\
&= \frac{1}{2}\int_0^1 dx \int_0^{1-x} dy \Big\{ +Y_R^{jf} Y_L^{fi} \log\Delta - \frac{1}{\Delta}\big(m_i m_j z^2 Y_L^{jf} Y_R^{fi}\big) \\
&\quad - \frac{1}{\Delta}\Big[m_f m_j z Y_L^{jf} Y_L^{fi} + m_f m_i z Y_R^{jf} Y_R^{fi} + \big(q^2 xy + m_f^2\big) Y_R^{jf} Y_L^{fi} \Big] \Big\},
\end{aligned}
\tag{33}
$$

where $\Delta \equiv z m_h^2 - xz m_j^2 - yz m_i^2 + (x+y) m_f^2 - xyq^2$ and $z \equiv 1 - x - y$.

$$
\Gamma(\mu N \to eN) = \left| -\frac{e}{16\pi^2} c_R D + \tilde{g}_{LS}^{(p)} S^{(p)} + \tilde{g}_{LS}^{(n)} S^{(n)} + \tilde{g}_{LV}^{(p)} V^{(p)} \right|^2 + (L \leftrightarrow R)
\tag{34}
$$

Finally, the branching ratio of $\mu \to e$ conversion are obtained

$$
\mathcal{B}(\mu N \to eN) = \frac{\Gamma(\mu N \to eN)}{\Gamma_{\text{capt. } N}}.
\tag{35}
$$

Section 4

Numerical analysis

Numerical analysis: General case

Using $h \to e\mu$ and $h \to e\tau$ decay, we get following bounds

$$\sqrt{|Y_L^{e\mu}|^2 + |Y_R^{e\mu}|^2} < 7.2 \times 10^{-4}\,, \qquad \sqrt{|Y_L^{e\tau}|^2 + |Y_R^{e\tau}|^2} < 3.0 \times 10^{-3}\,, \tag{36}$$

at 95% CL. By combining the results from $B_s - \bar{B}_s$ mixing, $\mathcal{B}(B_s \to \mu^+\mu^-)$ and $\Gamma(h \to sb) < 1.4\,\mathrm{MeV}$, we have

$$\Gamma(h \to sb) < 0.17\,\mathrm{MeV},$$

at 95% CL. The following expression is obtained.

$$\frac{\mathcal{B}(B_s \to \ell_1\ell_2)}{\mathcal{B}(h \to \ell_1\ell_2)} \approx 2.1|\bar{Y}_{sb}|^2\,, \tag{37}$$

thus we have $\mathcal{B}(B_s \to e\mu) < 2.1 \times 10^{-9}$, $\mathcal{B}(B_s \to e\tau) < 3.7 \times 10^{-8}$, $\mathcal{B}(B_s \to \mu\tau) < 1.5 \times 10^{-8}$ at 95% CL. For $B_s \to e\mu$, our predicted upper limit is three times lower than the current LHCb bound $\mathcal{B}(B_s \to e\mu) < 6.3 \times 10^{-9}$.

Numerical analysis: General case

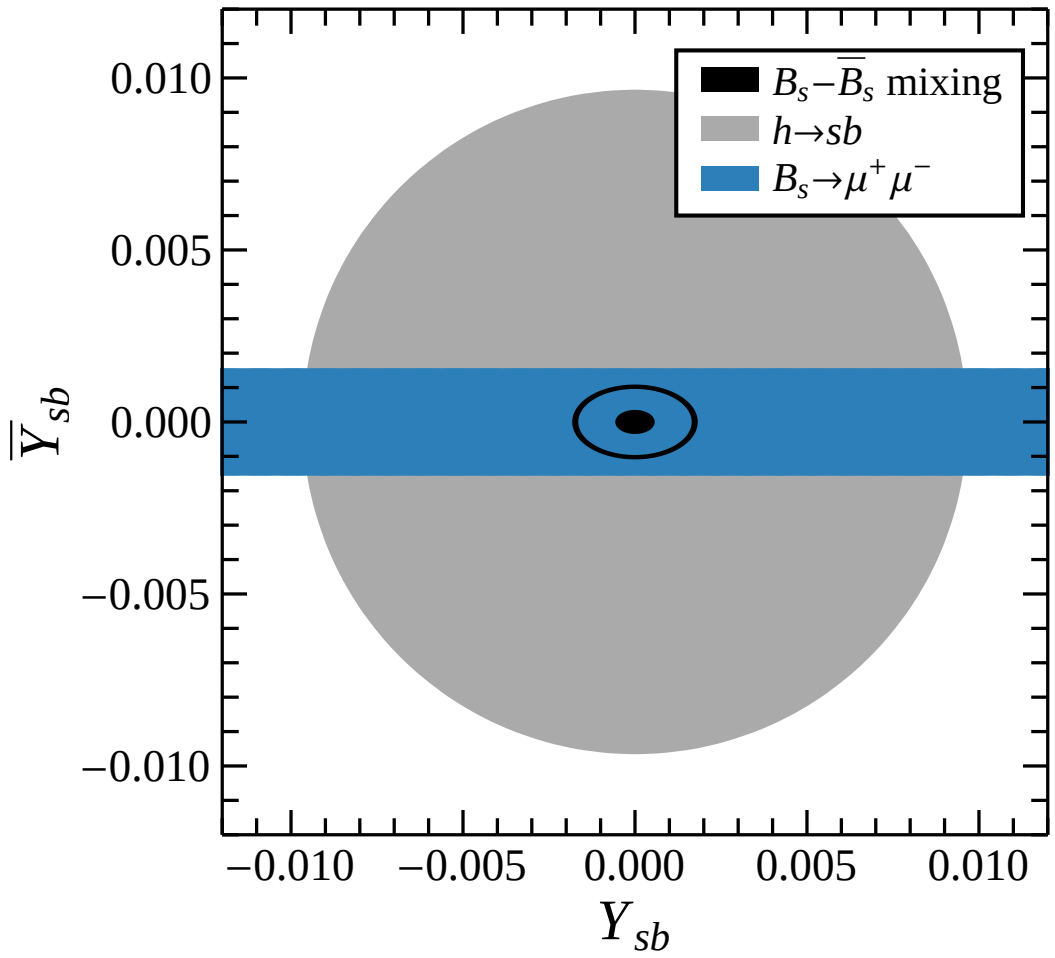

Figure: Allowed region of $(Y_{sb}, \bar{Y}_{sb})$ at 95% CL, assuming real Y_{sb} and $\bar{Y}_{sb}$ couplings. The blue region is allowed by $\mathcal{B}(B_s \to \mu^+\mu^-)$ with the assumption $(Y_{\mu\mu}, \bar{Y}_{\mu\mu}) = (Y_{\mu\mu}^{\rm SM}, 0)$. In the dark region, $\Gamma(h \to sb) < 1.4\,\mathrm{MeV}$.

Numerical analysis: Within Minimal Flavor Violation

In the MFV framework, we use below parameters for the lepton sector.

- $\mathcal{M} = 10^{15}\,\mathrm{GeV}$
- O = Identity matrix
- normal ordering (NO): $m_1 < m_2 < m_3$, $m_1 = 0$
- inverted ordering (IO): $m_3 < m_1 < m_2$, $m_3 = 0$

Finally, the Higgs Yukawa couplings in the MFV framework are determined by the following 6 real parameters

$$\left(\epsilon_0^u,\ \epsilon_0^d,\ \epsilon_1^d,\ \epsilon_0^\ell,\ \epsilon_1^\ell,\ \epsilon_2^\ell\right). \tag{38}$$

Then we have

- constraint on $(\epsilon_0^u,\ \epsilon_0^d,\ \epsilon_0^\ell)$, can be obtained by global fit of Higgs data
- ϵ_1^d by $B_s - \bar{B}_s$, $B_d - \bar{B}_d$ and $K^0 - \bar{K}^0$ mixing
- $(\epsilon_1^\ell,\ \epsilon_2^\ell)$ by the flavor-changing couplings for charged leptons

Numerical analysis: Within Minimal Flavor Violation

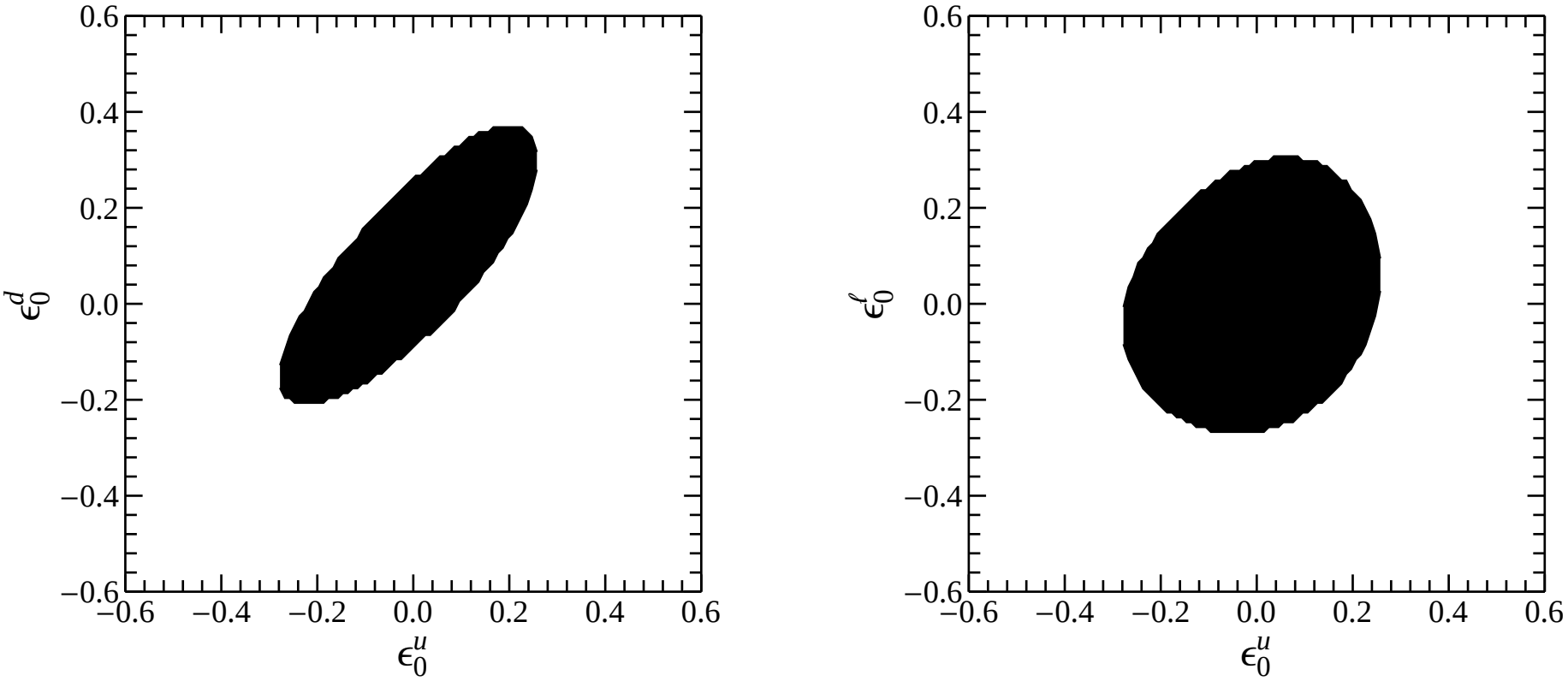

Figure: Allowed region of $(\epsilon_0^u,\, \epsilon_0^d,\, \epsilon_0^\ell)$ by the LHC Higgs data at 90% CL, plotted in the $(\epsilon_0^u,\, \epsilon_0^d)$ (left) and $(\epsilon_0^u,\, \epsilon_0^\ell)$ (right) plane.

Numerical analysis: Within Minimal Flavor Violation

The strong constraint is obtained

$$|\epsilon_1^d| < 0.59, \tag{39}$$

at 95% CL which results in

$$\begin{aligned} \Gamma(h \to sd) &< 7.4 \times 10^{-11}\,\mathrm{MeV}, \\ \Gamma(h \to sb) &< 2.0 \times 10^{-3}\ \mathrm{MeV}, \\ \Gamma(h \to db) &< 9.4 \times 10^{-5}\ \mathrm{MeV}, \end{aligned} \tag{40}$$

at 95% CL. At a centre-of-mass energy $500\ \mathrm{GeV}$ with an integrated luminosity of $4000\ \mathrm{fb}^{-1}$, ILC can provide a discovery sensitivity of 0.5% for $\mathcal{B}(h \to bj)$, with j representing a light quark, which is still about one order of magnitude larger than these upper limits listed above.

Numerical analysis: Within Minimal Flavor Violation

When deriving the bounds on these parameters and studying their effects, it's useful to separate from the effects of the quark Yukawa couplings. Therefore, we consider the following two scenarios in the discussion of the LFV processes.

$$\begin{aligned} &\text{Scenario I}: -0.5 < \epsilon^{\ell}_{0,1,2} < +0.5, \quad \text{Scenario II}: -1.0 < \epsilon^{\ell}_{0,1,2} < +1.0, \\ &\epsilon^{u}_{0} = \epsilon^{d}_{0} = 0, \qquad\qquad -1.0 < \epsilon^{u,d}_{0} < +1.0. \end{aligned} \tag{41}$$

We consider various LFV processes including $h \to \ell_i \ell_j$, $\ell_i \to \ell_j \ell_k \bar{\ell}_l$, $\ell_i \to \ell_j \gamma$, $\mu \to e$ conversion in nuclei, leptonic EDM, and anomalous magnetic moment.

Numerical analysis: Within Minimal Flavor Violation

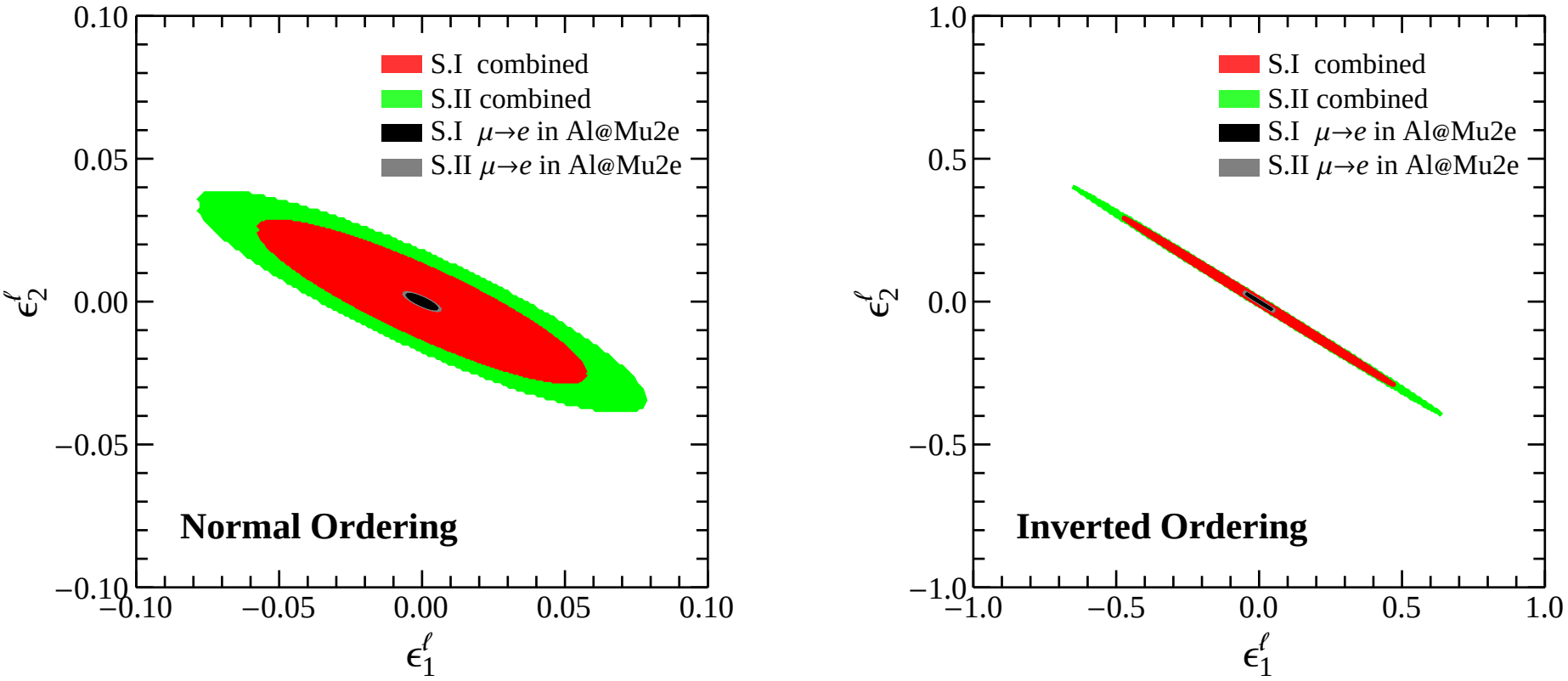

Figure: Combined constraints on $(\epsilon_0^u,\ \epsilon_0^d,\ \epsilon_0^\ell,\ \epsilon_1^\ell,\ \epsilon_2^\ell)$ at 90% CL, plotted in the $(\epsilon_1^\ell,\ \epsilon_2^\ell)$ plane, in the NO (Left) and IO (Right) cases, which are dominated by the $\mu \to e\gamma$ decay. The red and green regions are the allowed parameter space in Scenario I and II, respectively. The tiny black and dark regions indicate the future sensitivity to the $\mu \to e$ conversion in Al at the Mu2e experiment.

Numerical analysis: Within Minimal Flavor Violation

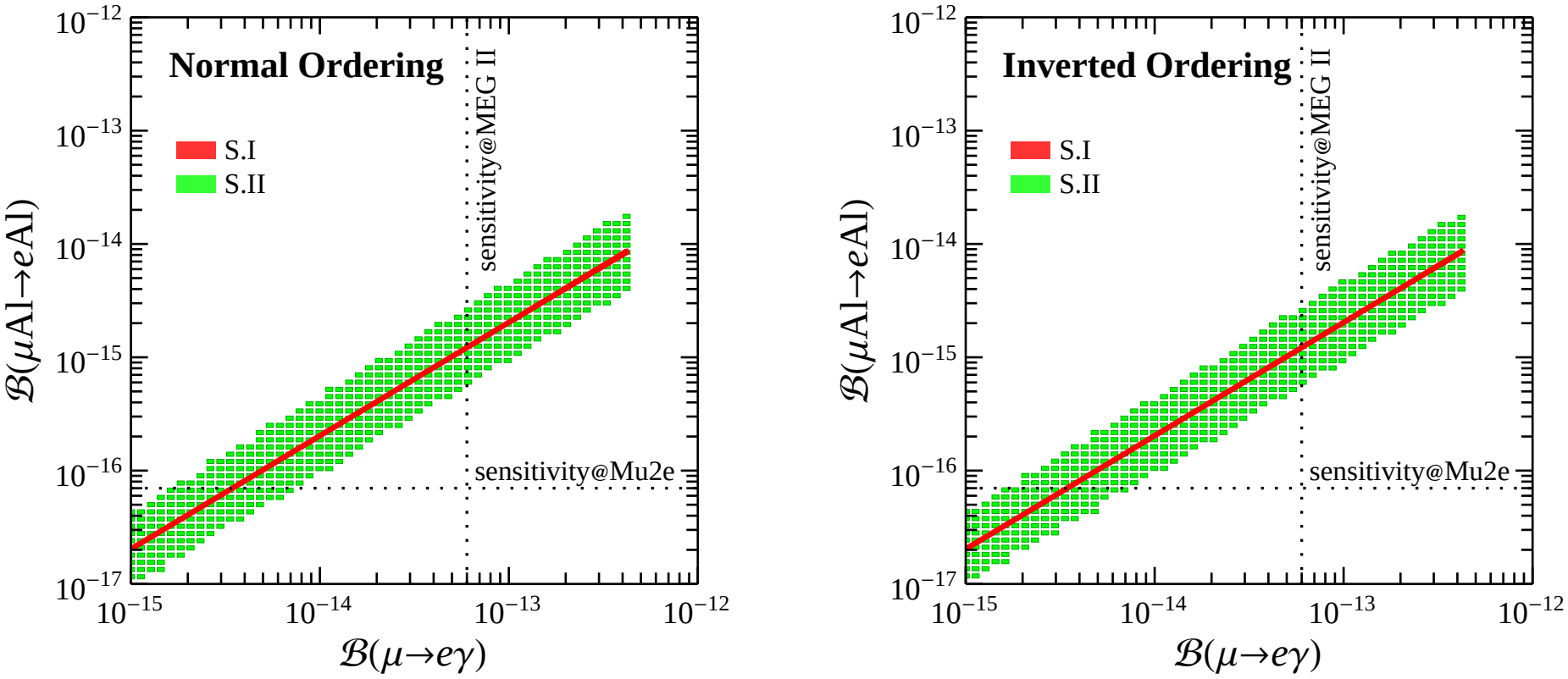

Figure: Correlation between $\mathcal{B}(\mu \to e\gamma)$ and $\mathcal{B}(\mu\text{Au} \to e\text{Au})$, in the NO (left) and IO (right) cases. The red and black region denotes the S.I and S.II, respectively.

Numerical analysis: Within Minimal Flavor Violation

		$\Gamma(h \to e\mu)$	$\Gamma(h \to e\tau)$	$\Gamma(h \to \mu\tau)$
NO	S.I	1.2×10^{-8}	1.3×10^{-5}	9.0×10^{-5}
NO	S.II	2.2×10^{-8}	2.4×10^{-5}	1.7×10^{-4}
IO	S.I	1.2×10^{-8}	4.7×10^{-6}	7.1×10^{-5}
IO	S.II	2.2×10^{-8}	8.7×10^{-6}	1.3×10^{-4}

		$\mathcal{B}(B_s \to e\mu)$	$\mathcal{B}(B_s \to e\tau)$	$\mathcal{B}(B_s \to \mu\tau)$
NO	S.I	2.4×10^{-16}	2.6×10^{-13}	1.8×10^{-12}
NO	S.II	4.6×10^{-16}	5.0×10^{-13}	3.5×10^{-12}
IO	S.I	2.4×10^{-16}	9.6×10^{-14}	1.4×10^{-12}
IO	S.II	4.5×10^{-16}	1.8×10^{-13}	2.6×10^{-12}

Table: Upper bounds on $\Gamma(h \to \ell_i \ell_j)$ [MeV] and $\mathcal{B}(B_s \to \ell_i \ell_j)$ at 90%CL.

Compare to the current experimental results from CMS
$\mathcal{B}(h \to e\mu) < 3.5 \times 10^{-4}$, $\mathcal{B}(h \to e\tau) < 6.1 \times 10^{-3}$,
$\mathcal{B}(h \to \mu\tau) < 2.5 \times 10^{-3}$ at 95% CL.

Section 5

Summary

Summary

- We study the tree-level Higgs FCNC interactions in the EFT approach, with and without MFV hypothesis.
- We investigate the Higgs FCNC effects on the $B_s - \bar{B}_s$, $B_d - \bar{B}_d$ and $K^0 - \bar{K}^0$ mixing, the lepton FCNC processes $\ell_i \to \ell_j \gamma$, $\ell_i \to \ell_j \ell_k \bar{\ell}_l$, $\mu \to e$ conversion in nuclei, the LHC Higgs data, and etc, and derive the bounds on the Higgs FCNC couplings.
- In the MFV hypothesis, we find that the bounds on $(\epsilon_0^u, \epsilon_0^d, \epsilon_0^\ell)$ are dominated by the LHC Higgs data, ϵ_1^d the $B_s - \bar{B}_s$ mixing, and $(\epsilon_1^\ell, \epsilon_2^\ell)$ the $\mu \to e\gamma$ decay.
- For the $B_s \to \ell_1 \ell_2$ and $h \to \ell_1 \ell_2$ decays, since the upper limits of their branching ratios are much lower than the current LHC bounds, searches for these LFV processes are very challenging at the LHC.
- With the improved measurements at the future MEG II and Mu2e experiments, searches for the LFV Higgs couplings in the $\mu \to e\gamma$ decay and $\mu \to e$ conversion in Al are very promising. In the MFV, the branching ratios of these two processes are strongly correlated to each other.

Backup

bkp 1

Here, $\tilde{g}^{(n,p)}_{L/RS,L/RV}$ denote the couplings to proton and neutron and can be evaluated from the quark-level ones

$$\tilde{g}^{(p)}_{LS,RS} = \sum_q g^q_{LS,RS} \frac{m_p}{m_q} f^{(q,p)}\,, \qquad \tilde{g}^{(p)}_{LV,RV} = g^q_{LV,RV}/Q_q\,,$$
$$\tilde{g}^{(n)}_{LS,RS} = \sum_q g^q_{LS,RS} \frac{m_n}{m_q} f^{(q,n)}\,, \tag{42}$$

where the summation runs over all quark flavors $q \in \{u, d, s, c, b, t\}$, and the nucleon matrix elements $f^{(q,p)} \equiv \langle p|m_q \bar{q} q|p\rangle/m_p$ are numerically

$$f^{(u,p)} = f^{(d,n)} = 0.024, \quad f^{(c,p)} = f^{(b,p)} = f^{(t,p)} = \frac{2}{27}\Big(1 - \sum_{q=u,d,s} f^{(q,p)}\Big),$$
$$f^{(d,p)} = f^{(u,n)} = 0.033, \quad f^{(c,n)} = f^{(b,n)} = f^{(t,n)} = \frac{2}{27}\Big(1 - \sum_{q=u,d,s} f^{(q,n)}\Big),$$
$$f^{(s,p)} = f^{(s,n)} = 0.25. \tag{43}$$

bkp 2

The coefficients D, $V^{(p)}$, $S^{(p)}$, and $S^{(n)}$ denote overlap integrals of the muon, electron and nuclear wave function. For the Au and Al nuclei, their values read

$$\left(D, V^{(p)}, S^{(p)}, S^{(n)}\right) = \begin{cases} 0.1890, 0.0974, 0.0614, 0.0918, & \text{for Au}, \\ 0.0362, 0.0161, 0.0155, 0.0167, & \text{for Al}, \end{cases} \tag{44}$$

in unit of $m_\mu^{5/2}$.

bkp 3

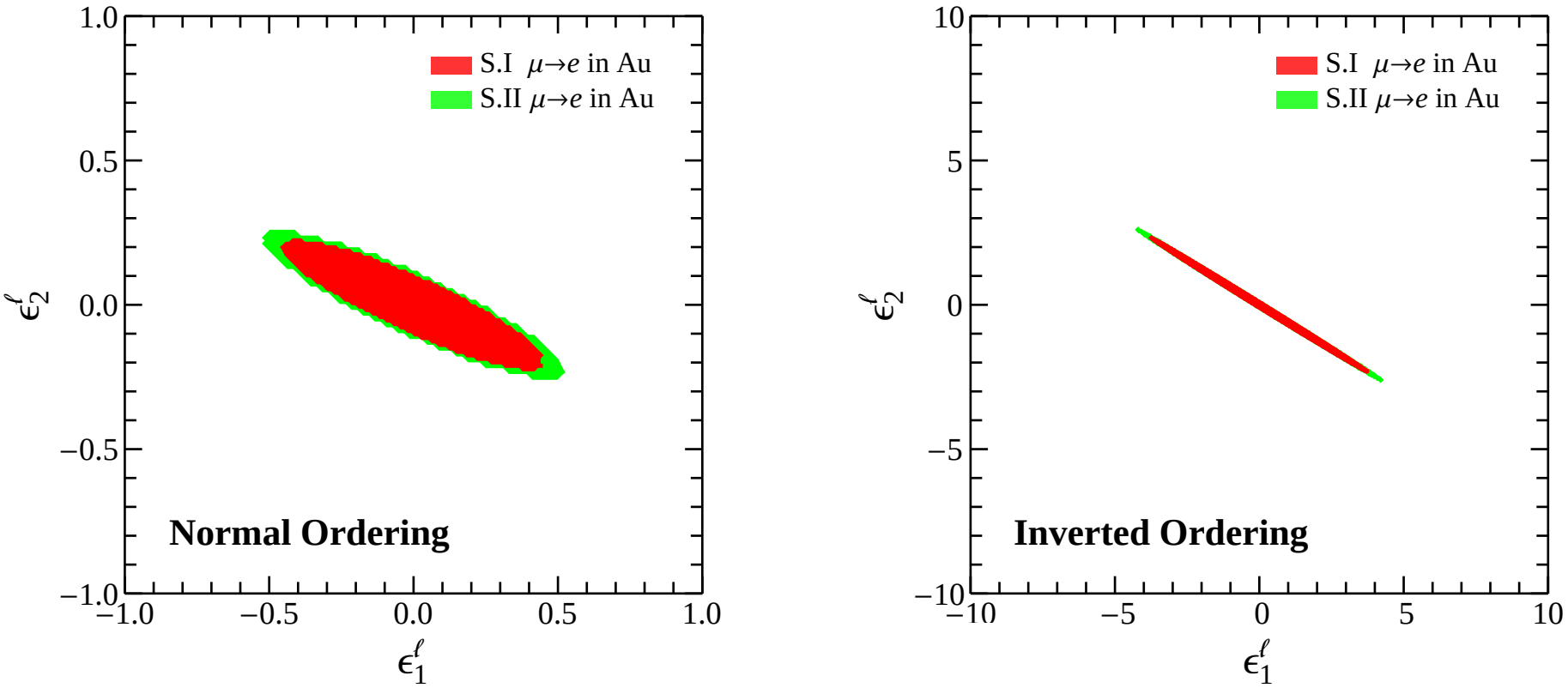

Figure: The same as Fig. 3, but only under the constraint of $\mu \to e$ conversion in Au.

bkp 4

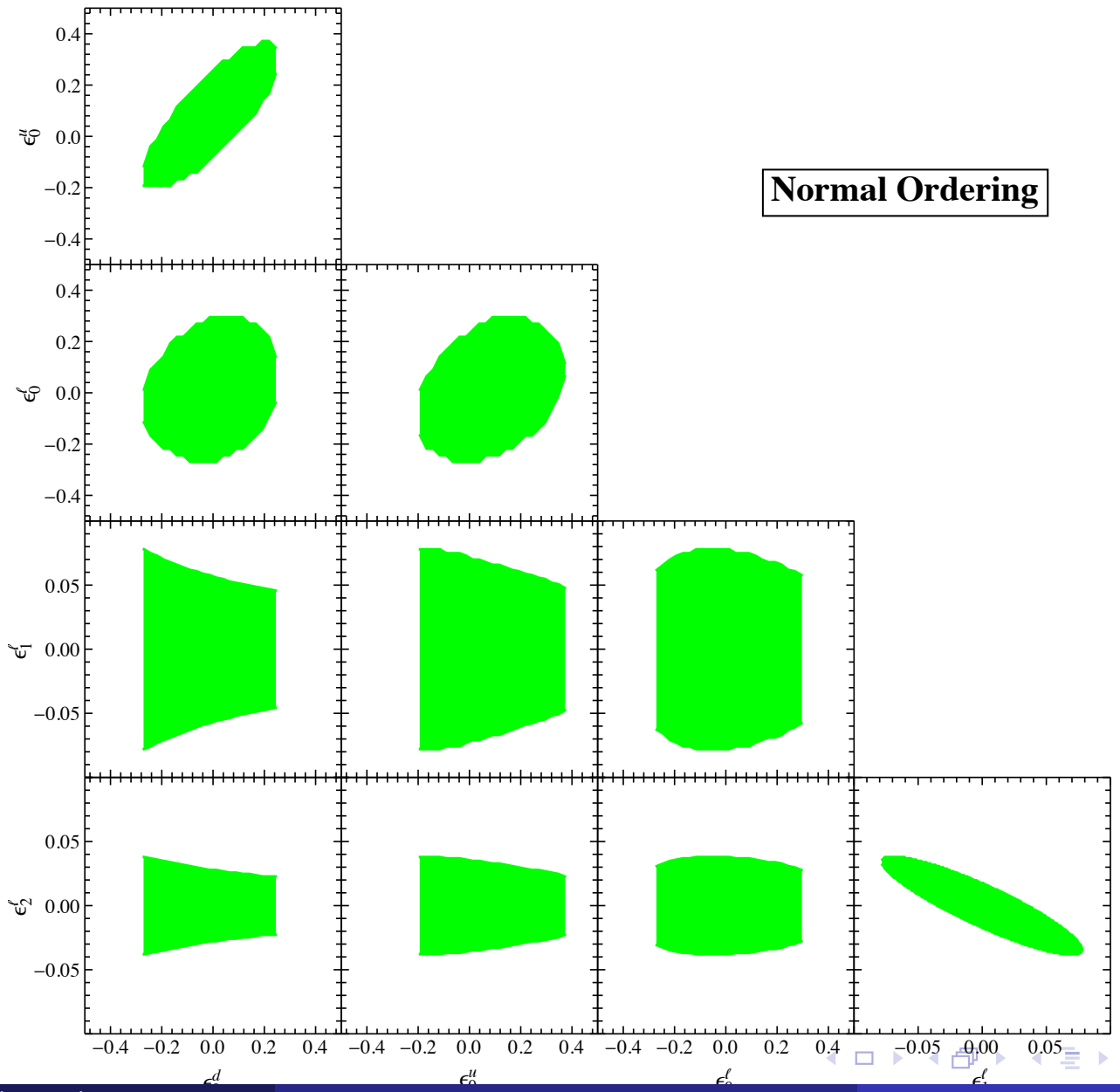
Normal Ordering
ϵ_0^u
ϵ_0^ℓ
ϵ_1^ℓ
ϵ_2^ℓ
ϵ_0^d
ϵ_0^u
ϵ_0^ℓ
ϵ_1^ℓ

bkp 5

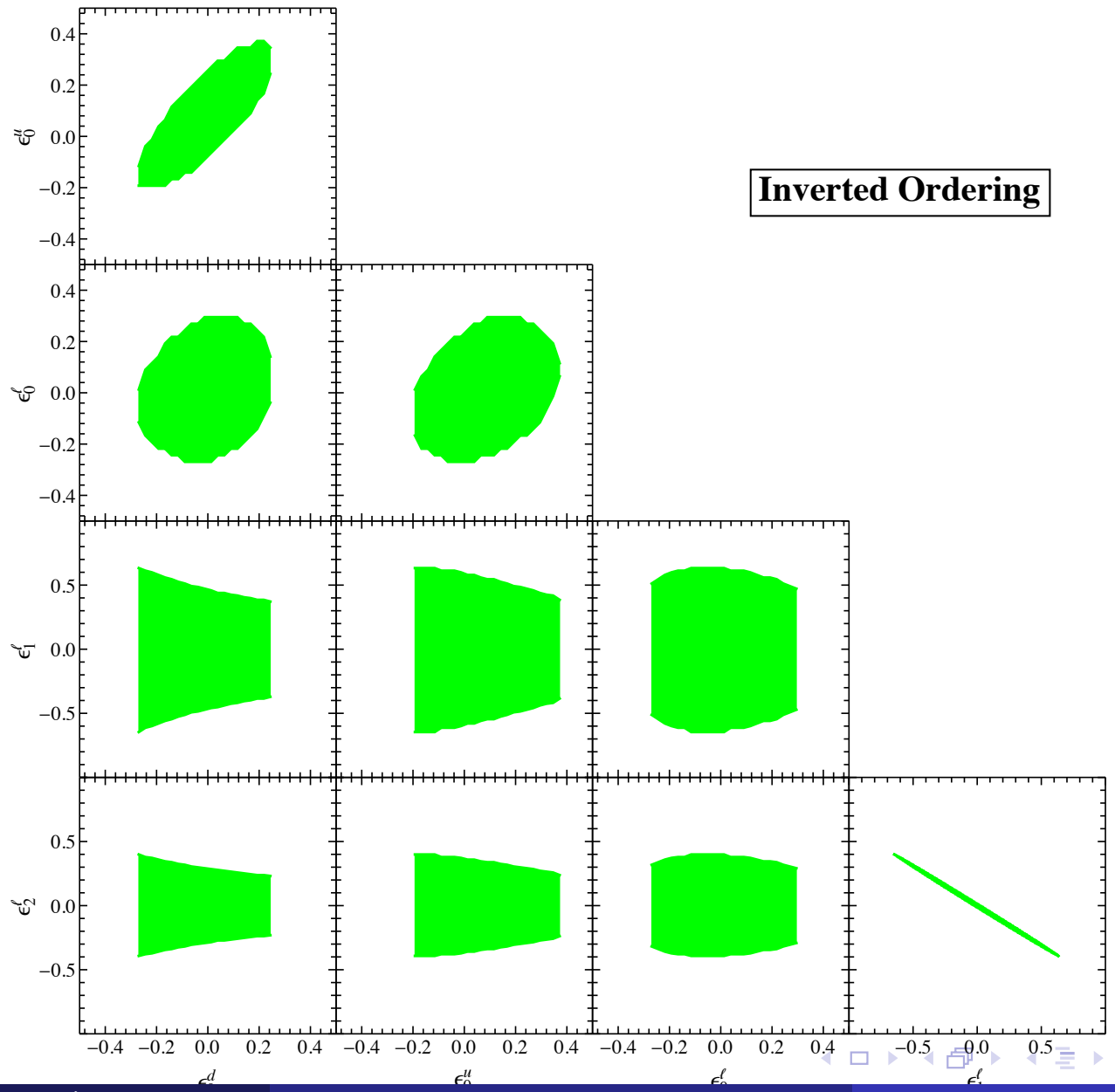
Inverted Ordering
ϵ_0^u
ϵ_0^ℓ
ϵ_1^ℓ
ϵ_2^ℓ
ϵ_0^d
ϵ_0^u
ϵ_0^ℓ
ϵ_1^ℓ